Identifying the Integrated Neural Networks Involved in Capsaicin-Induced Pain Using fMRI in Awake TRPV1 Knockout and Wild-Type Rats

[1]Jason R. Yee, [1]William Kenkel, [1]John C. Caccaviello, [3]Kevin Gamber, [3]Phil Simmons, [2]Mark Nedelman, [1]Praveen Kulkarni, [1]Craig F. Ferris

[1] Northeastern University, Center for Translational NeuroImaging, Boston MA; [2]Ekam Imaging, Boston MA, [2]SAGE Labs, St. Louis, MO

Abstract

In the present study, we used functional MRI in awake rats to follow the pain response that accompanies intradermal injection of capsaicin into the hindpaw. To this end, we used BOLD imaging together with a 3D segmented, annotated rat atlas and computational analysis to identify the integrated neural circuits involved in capsaicin-induced pain. The specificity of the pain response to capsaicin was tested in a transgenic knock-out of the TRPV1 receptor. This model contains a biallelic deletion of the TRPV1 gene, encoding for the transient receptor potential cation channel subfamily V member 1. Capsaicin is an exogenous ligand for TRPV1. As expected, capsaicin did not elicit the activation pattern in the TRPV1 knockout rats observed in wild-type controls. However, the intradermal injection of formalin elicited a significant activation of the putative pain pathway as represented by such areas as the anterior cingulate, somatosensory cortex, parabrachial nucleus and periaqueductal gray. Capsaicin in wild-type controls also activated the putative pain pathway in addition to brain areas involved in emotion and cognition.

Materials & Methods

Study and Imaging Protocols

Awake, male Sprague-Dawley (n=36; Charles River Laboratories) and TRPV1-KO rats (n=12; SAGE Laboratories) were challenged with capsaicin (1 mg/ml) (Material # M2028 Sigma-Aldrich, St Louis, MO) subdermal in the right hindpaw in a volume of 50 µl via a 27-gauge needle connected to PE 20 tubing extending from the bore of the magnet to a calibrated syringe. The same volume in the same hindpaw was given for formalin (3%) (source) or vehicle of 20% Captisol® (a modified β-cyclodextrin) in buffered saline (Ligand Pharmaceuticals, Inc. La Jolla, CA). Injections were separated by two weeks. All injection were performed in the magnet, under awake conditions during image acquisition. Experiments were conducted using a Bruker Biospec 7.0T/20-cm USR horizontal magnet (Bruker, Billerica, Massachusetts) and a 20-G/cm magnetic field gradient insert (ID = 12 cm) capable of a 120-µs rise time (Bruker). At the beginning of each imaging session, a high-resolution anatomical data set was collected using the RARE pulse sequence (22 slice; 1.0 mm; field of vision [FOV] 3.0 cm; 256 × 256; repetition time [TR] 2.5 sec; echo time [TE] 12.4 msec; NEX 6; 6.5 minute acquisition time. Functional images were acquired using a multi-slice HASTE pulse sequence (Half Fourier Acquisition Single Shot Turbo Spin Echo). A single scanning session acquired 22 slices, 1.0 mm thick, every 6.0 seconds (FOV 3.0 cm, matrix size 96 x 96, ETL 36, NEX 1) repeated 150 times for a total time of 15 minutes. Scanning session was continuous, starting with 50 baseline image acquisitions, then hindpaw injection followed by another 100 image acquisitions.

Imaging Analysis

Images were aligned and registered to a 3D rat brain atlas, which is segmented and labeled with 152 discrete anatomical regions. The alignment process was facilitated by an interactive graphic user interface. The registration process involved translation, rotation and scaling independently and in all three dimensions. Matrices that transformed each subject's anatomy were used to embed each slice within the atlas. All pixel locations of anatomy that were transformed were tagged with major and minor regions in the atlas. This combination created a fully segmented representation of each subject within the atlas. The inverse transformation matrix [Ti]-1for each subject (i) was also calculated.

Experimental Design

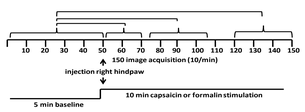

Shown are the statistical comparisons of different image acquisitions compared to baseline. A non-parametric Kruskal-Wallis test statistic was used to compare the average signal intensity in each of ca 15,000 voxel for their first 5 minutes baseline (acquisitions 1-50) to minutes 1-2 (acquisitions 51-71), minutes 3-5 (acquisitions 75-105), and min 8-10 (acquisitions 121-150) post capsaicin and formalin.

Bruker BioSpec 7T / 20cm USR

Quad transmit/receive volume coil built into the head holder

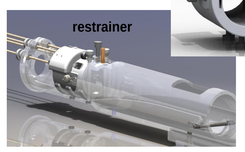

Optimal signal-to-noise and field homogeneity

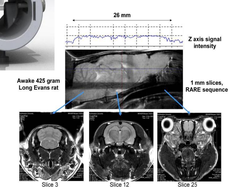

Studies were performed with a quad transmit/receive head coil and rat restrainer developed by Animal Imaging Research, Holden, Massachusetts

Main Results

Volume of Activation - Positive BOLD -3-5 Min

Region of Interest	Vehicle med	Vehicle max	Vehicle min	Capsaicin med	Capsaicin max	Capsaicin min	P value
central amygdala	0	1	0	10	19	3	0.001
tegmental nucleus	0	1	0	3	9	1	0.001
temporal ctx	3	9	0	25	46	12	0.001
parietal ctx	1	2	0	4	8	2	0.001
entorhinal ctx	15	23	5	99	168	53	0.001
basal amygdala	0	2	0	6	23	2	0.001
medial amygdala	0	3	0	9	13	2	0.001
insular ctx	2	6	0	15	38	3	0.001
ventral medial hypothalamus	3	8	0	16	21	7	0.001
auditory ctx	1	6	0	22	36	3	0.001
lateral amygdala	1	2	0	6	10	1	0.001
visual ctx	10	30	2	49	96	13	0.001
somatosensory ctx primary	8	41	0	97	195	19	0.001
somatosensory ctx secondary	2	13	0	26	66	2	0.002
motor secondary ctx	30	57	8	78	130	22	0.002
agranular insular ctx	3	13	0	21	56	2	0.002
gustatory ctx	1	6	0	17	41	1	0.003
periaqueductal gray midbrain	10	23	1	28	46	8	0.003
medial dorsal thalamus	3	11	0	12	15	3	0.003
bed nucleus stria terminalis	0	11	0	5	25	1	0.004
habenula thalamus	1	3	0	5	9	0	0.004
lateral hypothalamus	7	14	0	34	54	7	0.005
infralimbic ctx	1	6	0	9	19	1	0.005
ventral lateral striatum	1	18	0	12	34	2	0.005
parabrachial nucleus	2	6	0	11	15	2	0.005
dentate gyrus hippocampus	10	16	2	38	59	1	0.005
paraventricular thalamic nuclei	3	9	0	9	11	3	0.006
motor ctx primary	17	44	2	37	82	18	0.006
midbrain reticular nucleus	8	16	1	24	47	6	0.007
medial preoptic area	3	10	0	11	27	1	0.008
retrosplenial ctx	13	42	0	40	73	4	0.009
lateral preoptic area	0	3	0	3	8	0	0.009
superior vestibular nucleus	3	18	0	20	33	4	0.01
CA3 hippocampus ventral	6	16	0	19	35	2	0.012
pontine reticular nucleus	5	14	0	19	28	4	0.012
lateral septal nucleus	11	23	2	25	36	10	0.013
subiculum hippocampus	13	29	4	50	87	5	0.015
substantia nigra reticularis	6	11	2	15	20	4	0.016
dorsal medial striatum	4	9	0	13	19	2	0.017
dorsal lateral striatum	2	16	0	11	24	2	0.021
ventral medial striatum	1	14	0	7	15	1	0.023
anterior cingulate ctx	5	14	0	14	31	2	0.023
ventral tegmental area	1	7	0	7	12	0	0.055
gigantocellular reticular n. pons	14	57	4	33	76	9	0.064

Areas comprising the **putative pain** circuit

Areas comprising the **habenular** system

Putative Pain Neural Circuit

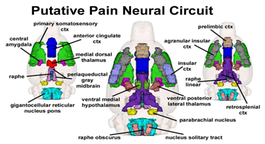

2D Axial Section

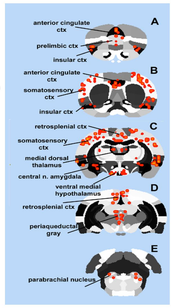

3D Coronal View

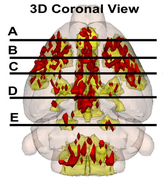

The putative pain neural circuit of the rat

Above The illustrations above show confluence of the segmented brain areas that make up the putative pain circuit (yellow/gold) as well as the location of the average significant increase (red) in BOLD signal for nine rats, 3-5 minutes after capsaicin injection into the right hind-foot. The panel of 2D axial images on the far right depict the location of significant increase in BOLD signal (red) in brain slices approximating the positions A-E shown in the 3D illustration.

Left A truncated list of 152 brain areas activated at 3-5 min post subdermal injection of vehicle and capsaicin in wild-type rats. The brain areas are rank ordered by significance. The voxel numbers were analyzed using a Newman-Keuls multiple comparisons test statistic.

Pain Neural Circuit

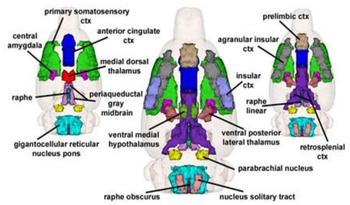

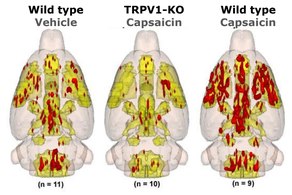

From Gaurau and Bernard, 2002

Cortical Loop of Papez

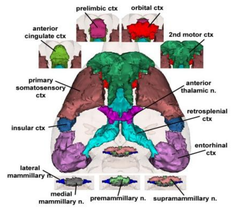

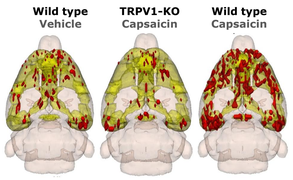

From Kulkarni et al, 2012

Habenular System

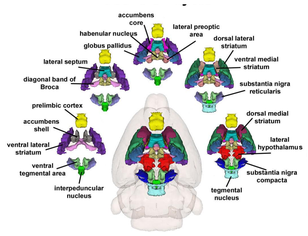

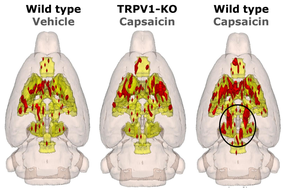

From Bianco and Wilson, 2009

Results

Region of Interest (ROI)	Vehicle med	Vehicle max	Vehicle min	Capsaicin med	Capsaicin max	Capsaicin min	Formalin med	Formalin max	Formalin min	P value
culmen cerebellum	21	68	3	1	4	0	40	96	6	0.001
lateral dorsal thalamus	1	9	0	0	0	0	3	16	1	0.002
medial dorsal thalamus	2	12	0	0	1	0	9	17	1	0.003
CA1 hippocampus ventral	4	34	0	0	1	0	13	67	2	0.003
paraventricular thalamic nuclei	5	11	3	0	2	0	5	11	0	0.004
superior vestibular nucleus	3	27	0	0	0	0	7	27	0	0.004
simple lobule cerebellum	8	49	0	0	6	0	25	97	2	0.005
declive cerebellum	8	47	0	0	0	0	21	43	0	0.005
anterior olfactory nucleus	0	14	0	0	2	0	5	38	3	0.006
paramedian cerebellum	11	44	0	0	0	0	1	34	0	0.006
periaqueductal gray midbrain	6	37	1	0	4	0	10	60	0	0.009
parafloccculus cerebellum	8	23	2	0	5	0	14	40	0	0.009
auditory ctx	2	9	0	0	0	0	6	98	0	0.009
motor ctx primary	10	68	2	8	15	0	31	133	10	0.011
nucleus lateral lemniscus	3	11	0	0	2	0	7	15	0	0.016
motor secondary ctx	18	97	1	6	24	0	59	139	7	0.017
anterior thalamic nuclei	5	11	0	0	3	0	8	20	1	0.017
CA3 hippocampus dorsal	11	16	0	1	2	0	8	26	5	0.018
parietal ctx	1	5	0	0	0	0	4	41	0	0.018
ansiform cerebellum	10	76	0	0	4	0	20	122	0	0.021
habenula thalamus	1	5	0	0	2	0	3	9	0	0.021
visual ctx	7	86	2	0	23	0	40	239	0	0.021
superior colliculus	23	77	1	2	9	0	38	107	0	0.024
diagonal band of Broca	0	2	0	0	1	0	2	5	0	0.024
temporal ctx	2	12	0	0	4	0	10	108	0	0.027
somatosensory ctx primary	14	119	1	5	7	1	62	347	3	0.031
somaotsensory ctx secondary	1	11	0	0	1	0	14	67	0	0.034
retrosplenial ctx	16	72	0	2	6	0	22	117	0	0.035
CA3 hippocampus ventral	9	22	0	1	2	0	9	38	0	0.036
accumbens shell	1	4	0	0	2	0	3	19	0	0.037
prelimbic ctx	0	19	0	3	6	0	6	39	2	0.041
subiculum hippocampus	3	41	0	1	9	0	20	117	0	0.043
tenia tecta ctx	1	5	0	1	7	0	6	19	0	0.045
dentate gyrus hippocampus	12	29	0	0	9	0	11	68	0	0.045
lateral septal nucleus	2	23	0	0	5	0	10	35	0	0.048
olfactory tubercles	9	21	0	3	8	1	22	36	1	0.049
central lobule cerebellum	1	81	0	3	22	0	43	97	2	0.055
gigantocellular reticular nucleus pons	12	93	0	0	9	0	8	52	0	0.061
piriform ctx	26	86	2	5	32	2	18	160	6	0.061
orbital ctx	0	8	0	1	2	0	5	25	0	0.065
interpeduncular nucleus	0	2	0	0	0	0	1	6	0	0.066
anterior cingulate ctx	3	33	0	4	5	0	8	56	1	0.071

Areas comprising the **putative pain** circuit

Areas comprising the **habenular** system

TRIPV1-KO rats' response to injections

A truncated list of 152 brain areas at 3-5 min post intradermal injection of **vehicle, capsaicin and formalin** into the hindpaw of TRPV1 knockout rats. The brain areas are rank ordered by significance. The voxel numbers for all time points were analyzed using a Newman-Keuls multiple comparisons test statistic.

BOLD timecourse in anterior cingulate cortex

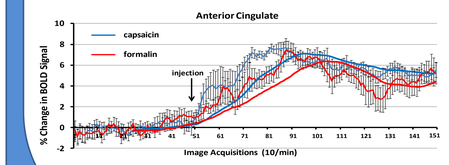

Percent change in BOLD signal over a 10 min period (acquisitions 51-150) following capsaicin in wild-type controls (blue) and formalin injection in TRPV1 KO rats (red). The anterior cingulate cortex, a key area in the pain neural circuit, shows a maximal change in BOLD signal within 3-5 min post injection of capsaicin or formalin. Trend lines (solid blue and red). Vertical lines denote SEM .

Conclusions

Functional neuroimaging of BOLD responses to painful stimuli in un-anaesthetized, awake animals effectively identified brain regions that have previously been demonstrated to mediate neural responses to pain, corroborating past work with a novel experimental approach.

Our data suggest that neuroimaging of pain in awake, conscious animals has the potential to inform the neurobiological basis of full and integrated perceptions of pain which, as we show here, recruit both affective and learning systems in addition to areas subserving sensorimotor aspects of pain perception.

Areas comprising the cortical loop described by Papez, and thought to play an important role in communicating affective information with subcortical limbic areas, were activated by capsaicin in wild-type rats, but displayed low activation levels equivalent with vehicle-treated wild-type rats in capsaicin-treated TRPV1-KO rats.

Areas comprising the habenular system, and thought to play an integrative role in aversive learning, were activated by capsaicin in wild-type rats, but displayed low activation levels equivalent with vehicle-treated wild-type rats in capsaicin-treated TRPV1-KO rats.

Formalin, which activates TRPA1 pain receptors, was capable of activating BOLD responses in areas that regulate conscious pain perception in TRPV1-KO rats, demonstrating that the specificity of a genetic manipulation of pain, i.e. eliminating only TRPV1-mediated pain, can be corroborated by differential BOLD activation patterns in the brain.